BEAM LOSS ESTIMATION BY MEASUREMENT OF SECONDARILY PRODUCED PHOTONS UNDER HIGH AVERAGE-CURRENT OPERATIONS OF COMPACT ERL IN KEK

H. Matsumura[†], A. Toyoda, S. Sakanaka, K. Haga, T. Obina, T. Miura, K. Hozumi,
S. Nagaguro, T. Oyama, KEK, Tsukuba, Ibaraki 305-0801, Japan
N. Yoshihara, Tokyo Nuclear Service Co., Ltd., Tsukuba, Ibaraki 300-2646, Japan

Abstract

To increase the beam current in the Compact Energy Recovery Linac (cERL) at the High Energy Accelerator Research Organization (KEK), the beam loss must be reduced to less than 0.01% during the transportation of 20 MeV electrons in order to suppress the radiation dose outside the accelerator room. Beam loss locations were successfully identified using the gold activation method, and the beam loss rate was estimated by comparing the measured dose rate with the simulated dose rate on the roof of the cERL room. Beam operation with beam current of 0.90 mA was achieved with a beam loss rate of less than 0.01%.

INTRODUCTION

The Compact Energy Recovery Linac (cERL)—an electron accelerator with a maximum energy of 26 MeV—has been under development at the High Energy Accelerator Research Organization (KEK), Tsukuba, Japan. The first successful energy recovery operation was conducted in 2014; subsequently, in 2015, the beam energy and current reached 20 MeV and 0.08 mA, respectively [1]. However, for the planned 1-mA operation, the beam loss must be less than 0.01% during the transportation of 20 MeV electrons to suppress the radiation dose outside the accelerator room installed cERL (cERL room). Therefore, detailed information about the beam loss was required. The beam loss locations were identified using the gold activation method, which is an offline measurement of ^{196}Au activity produced in gold foil attached to the surface of the beam duct by beam-loss-induced bremsstrahlung. Activity variation of ^{196}Au indicated the beam loss locations. The identified locations were then used for computer simulations of the beam loss. The beam loss rate was estimated by comparing the measured dose rate with the simulated dose rate on the roof of the cERL room. Based on the obtained beam loss information, the best beam transport conditions could be determined. In 2016, beam operation with beam current of 0.90 mA was achieved with a beam loss rate of less than 0.01%, subsequently, the beam current reached 0.95 mA.

IDENTIFICATION OF BEAM LOSS LOCATIONS

Gold Activation Method

In this study, the beam loss location for each beam operation was identified using the gold activation method.

† hiroshi.matsumura@kek.jp

The gold activation method has been used as a radiation monitor at high-energy accelerator facilities. Because this method, which uses the ^{197}Au(n, γ)^{198}Au reaction, has high sensitivity for thermal and epithermal neutrons, fluxes of thermal and epithermal neutrons have been measured in previous studies [2–4]. Spallation reactions in gold have also been used for high-energy hadron measurements [5–8]. In this study, a bremsstrahlung-induced reaction, ^{197}Au(γ, n)^{196}Au, was used for identifying the locations of electron beam loss for the first time.

Gold Foil Exposure to Bremsstrahlung

Gold activation experiments were performed four times: April 2, 2015 (EXP1), June 3–5, 2015 (EXP2), June 25, 2015 (EXP3), and February 26, 2016 (EXP4). Gold foils (thickness: 20 µm, diameter: 5.4 or 6.0 mm, chemical purity: 99.99%) were used as activation detectors. Each gold foil was packed in a polyethylene bag and attached to the surface of the recirculation loop beam duct. Typically, for one machine operation, 94 sheets (96 sheets for EXP1) of gold foil were installed 2-cm downstream from the edge of each magnet. As an example, the installation locations for EXP2, EXP3, and EXP4 are shown in Fig. 1.
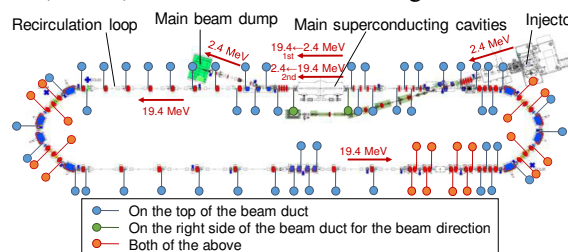

Figure 1: Outline of the electron acceleration and the gold foil installation positions for EXP2, 3, and 4.

After installing the gold foils, machine operation was performed. Beam current was monitored using a Faraday cup at the main beam dump. The net beam operation duration and its average beam current were 4.21 h and 28.8 µA for EXP1, 13.2 h and 5.42 µA for EXP2, 5.11 h and 51.2 µA for EXP3, and 1.78 h and 145 µA for EXP4, respectively. After acceleration by the main superconducting cavities, the kinetic energy of beam was 19.4 MeV.

Activity Determination of ^{196}Au in a Reference Gold Foil Using a Ge Detector

After the machine operation, the gold foils were retrieved from the cERL room. Then, the ^{196}Au absolute activity in one of the gold foils was determined as a refer-
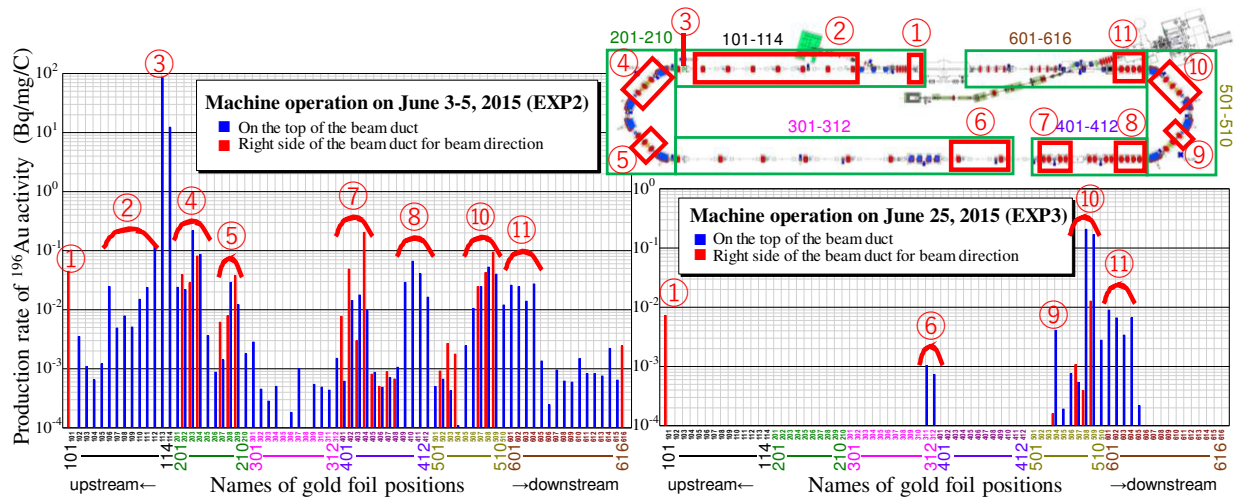
Figure 2: Examples of the production-rate distributions of ^{196}Au activity. The corresponding locations of the peaks indicated by numbers are shown on the accelerator map (top right).

ence using γ-ray spectrometry with high-purity Ge (HPGe) detectors. No ^{198}Au photo peaks, which are produced by neutron capture reactions, could be detected in the measured γ-ray spectra. The HPGe detectors were previously calibrated by Canberra [9]. The detection efficiencies of the HPGe detectors were determined using Canberra's LabSOCS software [10]. The nuclear data of ^{196}Au was obtained from literature [11], and the activity of ^{196}Au in the reference gold foil was used for calibrating the activity measurement using the imaging plate, as described in next section.

Activity Determination of ^{196}Au in the Gold Foil Using an Imaging Plate

All gold foils were removed from the polyethylene bags and taped to a sheet of paper with Scotch tape (3M, Scotch 810 Magic Tape or 3M, Scotch 811 Magic Removable Tape). Then, the gold foils were placed in contact with an imaging plate (Fujifilm, BAS SR2040) in order to expose the imaging plate to radiations from ^{196}Au produced in the gold foils. From the γ-ray spectrometry result described in the previous section, the ^{198}Au radiation contribution can be ignored. The radiation exposure to the imaging plate was performed in a 10-cm-thick lead shield box lined with 2-cm-thick copper and 0.5-cm-thick acrylic plates for 166, 96, 16.7, and 18.5 h in EXP1, EXP2, EXP3, and EXP4, respectively.

After imaging plate exposure, the imaging plate was scanned by a laser scanner for imaging (General Electric, Typhoon FLA 7000) to measure the relative photo-stimulated luminescence (PSL) values. The PSL read area was the same for all foils and was slightly smaller than the foil size to avoid depending on gold foil diameter. The relative PSL values indicate the relative activities of ^{196}Au in the gold foil. Finally, the relative activities were converted to absolute activities by normalizing them to the absolute activity of the reference gold foil. Subsequently,

we obtained the production rates of the ^{196}Au activity using the absolute activities.

Examples of the production-rate distributions of the ^{196}Au activity in the gold foils are shown in Fig. 2. In EXP2, many strong gold activation locations were observed over the recirculation loop. However, after improving the beam control, the number of beam loss locations and rates were drastically reduced from EXP2 to EXP3. The details are presented in [12]. In EXP4, from the gold activation result, beam improvement further reduced the beam loss.

Activation of the Beam Ducts

On the day after the EXP1 machine operation was performed, a beamline activation survey was carried out using a NaI(Tl) scintillation survey meter (Aloka, TCS-171B). Strong activation (contact dose rate: 14 μSv/h) of a copper beam collimator and weak activation (contact dose rate: 0.04-0.9 μSv/h) of stainless steel beam ducts could be found. The beam duct activation locations agreed with the gold foil activation locations.

With a LaBr$_3$ scintillation spectrometer (Canberra, IN1KL-1), γ-ray spectra from activated materials were obtained. The radionuclide produced in the collimator was identified as ^{64}Cu. On the other hand, radionuclides in the beam ducts were identified as ^{57}Ni and ^{51}Cr. From the reduction of the contact dose rate from the beam duct, most of the dose was contributed from γ rays from ^{57}Ni. Because the half-life of ^{57}Ni is 36 h, the memory of beam loss is retained for a few days. However, the sensitivity of the beamline survey was not sufficient for 0.01% beam loss.

ESTIMATION OF BEAM LOSS RATES

Dose Rate on the Roof of the cERL Room

The concrete roof of the cERL room is 100-cm thick, which is the thinnest shield wall of the cERL room. Therefore, secondarily produced photons can easily pene-

trate the roof. We suggest that the dose rate on the roof of the cERL room is appropriate for estimating the beam loss rate. First, the dose rates on the roof were measured along the beamline. Second, the dose rate corresponding to 1-nA beam loss was calculated using the MARS15 code [13]. Finally, beam loss rates were estimated by comparing the measured dose rate with the calculated dose rate. The details are described below.

Measurement of Dose Rates on the Roof

During machine operation for the gold activation experiments, the photon dose rate on the roof of the cERL room was measured by a NaI(Tl) scintillation survey meter (Aloka, TCS-161 or TCS171B). The measurement was performed by walking on the roof of cERL room along the recirculation loop. The dose rate was increased slightly downstream from the beam loss locations identified by the gold activation method.

Calculation of Dose Rates on the Roof

The photon dose rate was calculated by the MARS15 code [13]. In the case of beam loss at the electric magnet, 20-MeV electrons were bombarded with the beam duct on the inner surface at upward 1° in the center of the electric magnet. In the case of beam loss at the collimator, 20-MeV electrons were bombarded with the collimator in the beam direction.
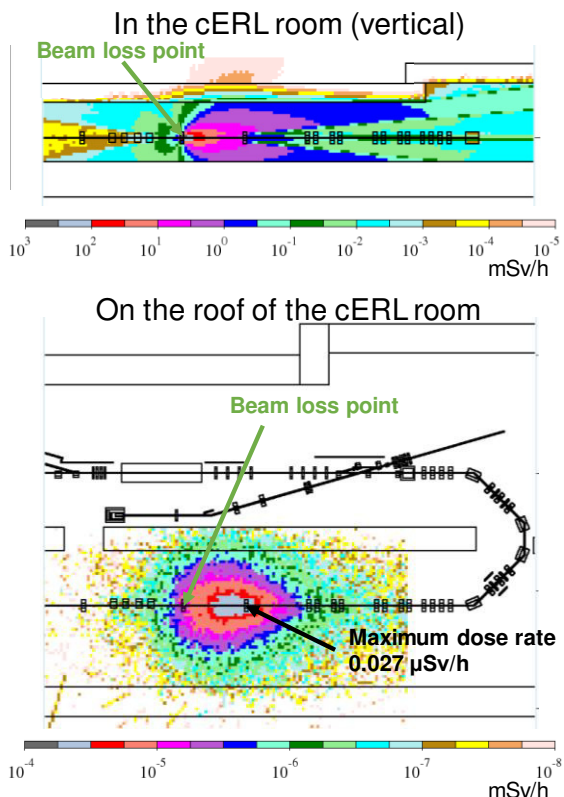

Figure 3: Example of the dose rate distribution calculated using MARS15. In this calculation, 1-nA beam loss occurred in the center of the electric magnet (QMIL03).

An example of the MARS15 calculation result is shown in Fig. 3. The maximum dose rate appeared slightly downstream of the beam loss point, as observed in the measurement. In this case, a beam loss of 1 nA leads to a dose rate of 0.027 µSv/h on the roof of the cERL room. Using the measured and calculated dose rates, the beam loss rate can be estimated.

Estimated Beam Loss Rates

Beam loss rates were estimated by comparing the measured and calculated dose rates on the roof of the cERL room. An example of the beam loss rates is shown in Fig. 4. The beam loss rates were obtained at EXP3. All beam loss rates were found to be much lower than 0.01% of the beam that had been transferring in the recirculation loop. This result allowed higher current operation up to 1 mA.
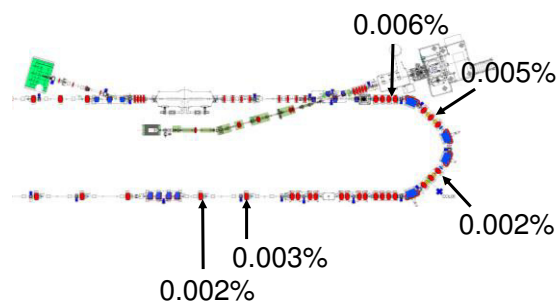

Figure 4: Beam loss rates estimated from the measured dose rates on the roof of the cERL room for EXP3.

In 2016, the beam current reached 0.90 mA. The dose rate on the roof of the cERL room during 0.90-mA beam operation is presented by S. Sakanaka *et al.* [12]. The maximum dose rate was 3.8 µSv/h at a collimator in the first arc section (COL4). From the dose rate, the beam loss rate was estimated to be 0.009%. In the south-straight section (opposite side of main-linac) of the recirculation loop, 0.05 µSv/h is the highest dose rate around an electric magnet (QMIM01). The dose rate corresponds to a beam loss rate of 0.0002%. Very small beam loss operation was accomplished under high average-current (0.90-mA) operations of cERL in KEK. Immediately after the confirmation of the small beam loss rate, 0.95 mA beam current could be recorded as the best [12].

ACKNOWLEDGEMENT

REFERENCES

[1] S. Sakanaka *et al.*, "Recent Progress and Operational Status of the Compact ERL at KEK," in *Proc. IPAC'15*, Richmond, VA, USA, May. 2015, paper TUBC1, pp. 1359–1362.

[2] K. Masumoto, A. Toyoda, K. Eda, and T. Ishihara, "Measurement of the spatial distribution of neutrons in an accelerator room by the combination of activation detectors and an imaging plate," *Radiat. Safety Manag.*, vol. 1, pp. 12–16, 2002.

[3] Q. Wang *et al*., "KENS shielding experiment (2): Measurement of the neutron spatial distribution inside and outside of a concrete shield using an activation foil and an imaging plate technique," *J. Nucl. Sci. Technol.*, vol. 41, sup. 4, pp. 26–29, 2004.

[4] H. Matsumura *et al*., "Detailed spatial measurements and Monte Carlo analysis of the transportation phenomena of thermal and epithermal neutrons from the 12-GeV proton transport line to an access maze," *Nucl. Instr. Meth. B*, vol. 266, pp. 3647–3655, 2008.

[5] H. Matsumura *et al*., "Characteristics of high-energy neutrons estimated using the radioactive spallation products of Au at the 500-MeV neutron irradiation facility of KENS," *Radiat. Prot. Dosimetry*, vol. 116, pp. 1–5, 2005.

[6] H. Matsumura *et al*., "Indirect measurement of secondary-particle distributions by an Au activation method at the KEK neutrino target station," *J. Radioanal. Nucl. Chem.*, vol. 272, pp. 423–428, 2007.

[7] H. Matsumura *et al.*, "Shielding experiments under JAS-MIN collaboration at Fermilab (III): Measurement of high-energy neutrons penetrating a thick iron shield from the antiproton production target by Au activation method," *J. Korean Phys. Soc.*, vol. 59, pp. 2059–2062, 2011.

[8] H. Matsumura *et al*., "Material activation benchmark experiments at the NuMI hadron absorber hall in Fermilab," *Nuclear Data Sheets*, vol. 120, pp. 219–221, 2014.

[9] R. Venkataraman, F. Bronson, V. Atrashkevich, M. Field, and B. M. Young, "Improved detector response characterization method in ISOCS and LabSOCS", *J. Radioanal. Nucl. Chem.*, vol. 264, pp. 213–219, 2005.

[10] F. L. Bronson, "Validation of the accuracy of the LabSOCS software for mathematical efficiency calibration of Ge detectors for typical laboratory samples", *J. Radioanal. Nucl. Chem.*, vol. 255, pp. 137–141, 2003.

[11] R. B. Firestone, *Table of Isotopes, 8th ed.*, John Wiley and Sons, Inc., New York, 1996.

[12] S. Sakanaka *et al*., "Measurement and control of beam losses under high average-current operation of the compact ERL at KEK", presented at IPAC'16, Busan, Korea, May 2016, paper MOAB01, this conference.

[13] N. V. Mokhov and S.I. Striganov, "MARS15 overview," in *Proc. Hadronic Shower Simulation Workshop*, Batavia, IL, USA, Sep. 2006, *AIP Conf. Proc.* vol. 896, pp. 50–60, 2007.